Complete Redox Exchange of Indium for Tl^+ in Zeolite A. Crystal Structures of Anhydrous Tl_{12}−A and In_{10}−A·In. Indium Appears as In^{2+}, In^+, and In^0. The Clusters $(In_5)^{8+}$ and $(In_3)^{2+}$ Are Proposed

Nam Ho Heo,* Hee Cheul Choi, Sung Wook Jung, Man Park,† and Karl Seff*,‡

Department of Industrial Chemistry, Kyungpook National University, Taegu 702-701, Korea, Department of Agricultural Chemistry, Kyungpook National University, Taegu 702-701, Korea, and Department of Chemistry, University of Hawaii at Manoa, Honolulu, Hawaii 96822-2275

Received: January 2, 1997[⊗]

Indium has replaced all of the Tl^+ ions in fully dehydrated fully Tl^+-exchanged zeolite A by a solvent-free redox ion-exchange reaction with In metal at 623 K. The crystal structures of the zeolite before ($Tl_{12}Si_{12}Al_{12}O_{48}$: $a = 12.153(4)$ Å, $R_1 = 0.054$, and $R_2 = 0.060$) and after the reaction, followed by washing with water and redehydration at 623 K ($In_{10}Si_{12}Al_{12}O_{48}$·In: $a = 12.098(2)$ Å, $R_1 = 0.063$, and $R_2 = 0.062$), have been determined by single-crystal X-ray crystallography at 294 K using the space group $Pm3m$. In In_{10}−A·In, 11 In atoms or ions/unit cell are distributed over seven crystallographically distinct positions. Seven In ions occupy 3-fold-axis equipoints: four In^+ ions lie opposite 6-rings in large cavity (In(1)), and two In^{2+} (In(2)) and one In^+ (In(3)) lie opposite 6-rings in the sodalite unit. Three In^+ ions per unit cell are found at two different 8-ring positions: 1.5 on the 8-ring plane (In(4)) and 1.5 off (In(5)). Finally, one In^0 atom per unit cell, probably associated with In ions, is found at two quite unusual positions: one-half of an In^0 lies at the center of sodalite unit (In(6)) and the other half of the In^0 is opposite a 4-ring relatively deep in the large cavity (In(7)). The crystal structure of In_{10}−A·In is viewed as a mixture of two kinds of "unit cells," In_8−A·In and In_{12}−A·In, each with a cationic charge of 12+. By their approach distances to framework oxygens, the ionic radii of In^+ and In^{2+} are *ca.* 1.23 and 1.04 Å, respectively. The In(6) and In(7) positions lie deep within cavities where they approach only In cations. This suggests the existence of tetrahedral $(In_5)^{8+}$ clusters (four In^{2+} ions at In(2) with an In^0 atom at their center at In(6), In(2)−In(6) distance = 2.754(2) Å) in half of the sodalite units (In_8−A·In), and bent $(In_3)^{2+}$ clusters (In(1)−In(7)−In(1) angle = 148.0(9)° and In(1)−In(7) = 3.073(8) Å) in half of the large cavities (In_{12}−A·In).

Introduction

Inclusion of various chemical species of the group III−V elements, including ions, atoms, and clusters of Ga and In, into the three-dimensional channels and cavities of zeolites are of interest to many material scientists as routes or precursors for developing regular arrays of nanosized clusters of semiconductor materials.[1−11] They may also be good catalysts for potentially important chemical reactions.[12−18] Clusters of GaP synthesized in the cavities of zeolite Y by chemical vapor deposition techniques have been extensively studied for their promising quantum size effects.[3,4] Gallium species in ZSM-5, introduced by ion exchange[12] or by impregnation[13] of gallium salts or by reducing mechanical mixtures of Ga_2O_3 and the zeolite,[14] were found to be active for the aromatization of light alkanes[12,15] and for hydrocarbon reduction.[16,17]

Alekseev *et al.* have reported the physical inclusion of indium metal into the lattice of zeolite A at extreme conditions, such as 20 kbar of pressure, and the formation and possible structures of Na_{12}−A(8In) have been suggested.[19,20] Other In species, probably In^+ as claimed, of relatively small amount (*ca.* 3.66 wt % as oxide) have been introduced by Kanazirev *et al.* into zeolite ZSM-5 (Si/Al ratio in the composition of synthesis gel *ca.* 3.5) by mixing In_2O_3 and the zeolite, followed by reduction with hydrogen.[18] Uchida *et al.* have also reported the aqueous ion exchange of In^{3+} into mordenite (Si/Al ratio *ca.* 9.6); the extent of ion exchange was ≤71% (*ca.* 11.3 wt % of indium).[21] Numerous attempts to ion-exchange In^+ into zeolites of high Al content (lower Si/Al ratio), as routes to the formation of group III species in zeolite frameworks, have failed due to the loss of zeolite crystallinity that occurs at the very low pH values required to keep the group III cations in solution.[1,22] Other methods, including the use of melts of anhydrous nitrates and halides, have also failed for similar reasons.[1]

The In^+ ion is thermodynamically unstable with respect to disproportionation in aqueous solution.[23,24] Indium(I) chloride and bromide, prepared by solid-state reactions, readily dissolve in water with the formation of indium metal: $3In^+ \rightarrow In^{3+} + 2In^0$.[25] Even in dilute perchloric acid, In^+ is unstable at moderate concentrations, being slowly oxidized to In^{3+} by H^+.[26] Although In^+ is more stable toward disproportionation in acetonitrile than in aqueous solution, pure solutions readily become mixtures of In^+ and In^{3+}.[27]

In this work, solvent-free redox ion exchange[28−30] was attempted with the hope that the redox potential for the reaction, $Tl^+ + In^0 \rightarrow In^+ + Tl^0$ within zeolite A (Si/Al ratio probably 1.00, although reported to be a bit greater, *ca.* 1.04[31]), would be positive. If so, complete In^+ exchange, Tl_{12}−A + $12In^0 \rightarrow In_{12}$−A + $12Tl^0$ might occur without the problems frequently encountered in solution. Despite the small or negative values of ΔE°_{aq} for the reactions between Tl^+ and indium metal (In^0) (0.002, −0.066, and −0.190 V for the formation of In^{3+}, In^{2+}, and In^+, respectively),[32] the favorable difference in ionization potentials could allow one or more of these reactions to occur. Because the reactions are atomistic, and because the elemental reactant and product are either gases or highly mobile liquids at the reaction temperature, ionization potential differences may

† Department of Agricultural Chemistry.
‡ Department of Chemistry.
⊗ Abstract published in *Advance ACS Abstracts,* June 1, 1997.

S1089-5647(97)00206-X CCC: $14.00 © 1997 American Chemical Society

be better criteria of spontaneity for high-temperature solvent-free reactions in zeolites than ΔE°_{aq} values, which describe reactions between species in aqueous solution at 298 K. By this reasoning, the 31.0 kJ/mol difference in the first ionization potentials of Tl^0 and In^0 (589.3 and 558.3 kJ/mol, respectively)[33] would suggest that the above reaction should occur.

In the present work, a solvent-free ion-exchange reaction between In^0 and Tl^+ within fully dehydrated Tl_{12}−A was carried out with the hope that a high degree of exchange, perhaps complete exchange, would occur. Following electron-probe X-ray microanalyses (EPXMA), the crystal structures of reactant and product would be studied crystallographically. If indium exchange is accomplished, chemically reactive indium species may be generated in the cavities of zeolite A. Interesting clusters may form and be identified. Such a product may have immediate utility or be a precursor to useful materials.

Experimental Section

Single crystals of zeolite A ($Na_{12}Si_{12}Al_{12}O_{48}\cdot 27H_2O$, Na_{12}−A, or Na−A),[34] cubes 80 μm on each edge, were synthesized by Kokotailo and Charnell.[35] Fully Tl^+-exchanged zeolite A ($Tl_{12}Si_{12}Al_{12}O_{48}$, Tl_{12}−A, or Tl−A), was prepared by dynamic ion-exchange (flow method) of Na−A crystals with 0.1 M aqueous thallous acetate (pH = 6.4, Aldrich Chemical Co., 99.99%). This had been shown to be suitable for the preparation of stoichiometric Tl_{12}−A.[36,37] Several crystals of colorless Tl−A were completely dehydrated at 623 K and 1×10^{-6} Torr for 48 h (sample A for electron−probe analysis). One of these crystals, still under vacuum, was then sealed in its capillary with a small torch for X-ray structure determination (crystal 1).

The remaining crystals of fully dehydrated Tl−A were exposed to In^0 (Samchun Chemical Co., 99.99%) under vacuum in fine Pyrex capillaries at 623 K for 96 h. This was achieved by condensing In^0 on and near the crystals from an In metal source at 723 K in a coaxially connected heating oven. Although the vapor pressure of In(*l*) is reported to be very low at 623 K (*ca.* 2.92×10^{-10} N/m^2 = 2.19×10^{-12} Torr),[38] droplets of In were seen to form very close to the zeolite crystals. It is possible that In_2O(g), from the decomposition of In_2O_3 on the surface of the original In sample, mediated the transport of In to the zeolite crystals. (In_2O is volatile[39] and sublimes in the range 838−973 K.[40] Indium transport has been observed to be particularly facile in other zeolite systems.)[18]

The temperature of the In source was then lowered to below 623 K; after 24 h the In^0 droplets near the zeolite crystals were no longer seen. Except for the reversed temperature gradient during the reaction period (previous paragraph), other experimental procedures for the reaction were similar in detail to those previously described for solvent-free redox ion exchange.[28−30] The resulting crystals, still under vacuum in their capillaries, were pale yellow.

Four attempts were made to determine the structure of these pale yellow crystals crystallographically. In each case, the structure refined to reasonable final error indices (*R*s *ca.* 0.08), but the number of indium atoms or ions per unit cell ranged from 10 to 14 for reasons which were not apparent. These results do indicate, however, that these crystals contain far less scattering density than they would if they contained both all of their initial thalliums (as atoms or ions) and all of the indiums (as atoms or ions) found in the final crystal structure (crystal 2, *vide infra*). However, all of the In atoms and ions found in the final structure must have entered the zeolite during the previous reaction step (exposure to In). Therefore, at least most of the Tl^+ ions must have left the zeolite during this reaction step. Most if not all must have been reduced by In atoms as desired

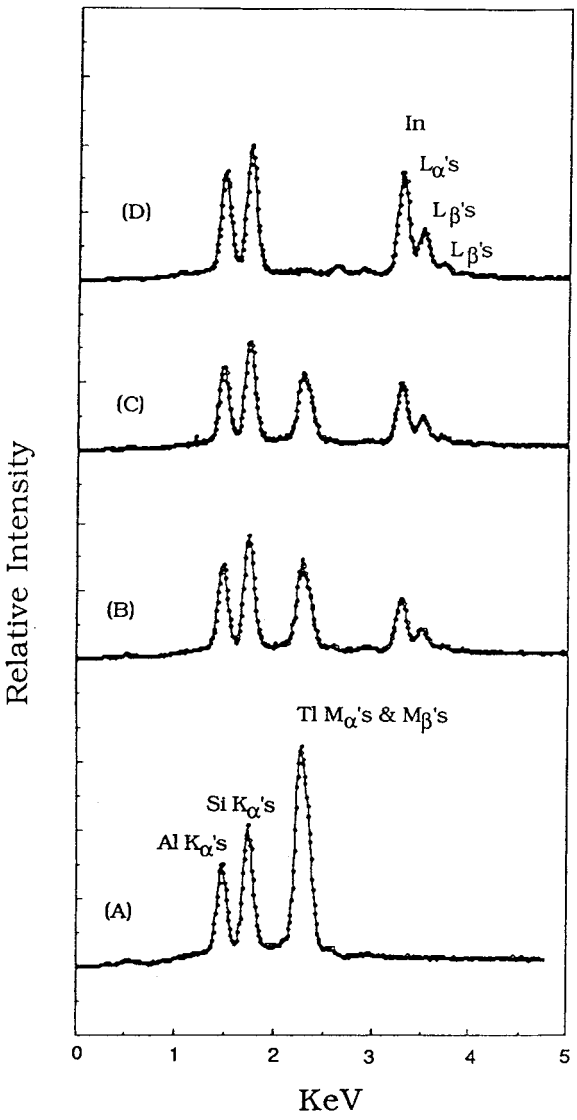

Figure 1. EPXMA spectra of Tl-A and of its reaction products with In metal: (A) examined after the consecutive treatments i-d-e (defined below), (B) i-d-r-e, (C) i-d-r-e-d-e, and (D) i-d-r-e-w-d-e. (i, ion-exchange with 0.1 M aqueous thallous acetate; d, dehydration at 623 K and 1×10^{-6} Torr for 48 h; e, exposure to the atmosphere at ambient conditions; r, reaction with In metal at 623 K for 96 h; and w, washing with deionized water at room temperature).

to give Tl^0, but a smaller fraction may have reacted with In_2O to give Tl_2O. Any Tl^0 and Tl_2O which could migrate to the crystal surface during the reaction (at 623 K) would have had sufficient vapor pressure to distill away. Because both Tl^0 and Tl_2O are black (Tl^0 may be dark lustrous if aggregated sufficiently), it is clear that none has remained on the surface of the clear pale yellow crystals.

When these crystals were exposed to the atmosphere for electron-probe analysis, they became lustrously black. Spectrum B in Figure 1 indicates a high thallium content for that sample. Perhaps small amounts of thallium remaining in the zeolite, atomically dispersed as Tl^0 or molecularly dispersed as Tl_2O, possibly in association with In ions, came to the surface upon exposure to the atmosphere, there to blacken the crystal and to be seen by EPXMA; both visual observation and EPXMA are surface sensitive techniques. The vapor pressure of Tl^0 is only 1.2×10^{-6} Torr at 623 K,[41] and atoms or small clusters stabilized within the zeolite might not readily vaporize. The vapor pressure of Tl_2O is greater (9.6×10^{-5} Torr),[42] but it may be more easily held within the zeolite because its oxide

ions can bridge. These neutral Tl species might well not be black when dissolved within the zeolite, but upon exposure they appear to have aggregated on the crystal surface. There the atmosphere apparently partly oxidized and hydrolyzed the Tl^0 and/or Tl_2O to give a mixture containing as many as all of the following Tl species: Tl^0, Tl_2O, Tl_2O_3 (all dark or black), TlOH, and $Tl(OH)_3$ (both colorless). Tl^+ positions may be very similar to those of In^+ in the zeolite, so small (and variable) amounts of Tl^+ may have been responsible for the erratic crystallographic results described in the previous paragraph.

Whether these black crystals were then washed or not, they became colorless upon dehydration and remained colorless upon later rehydration. If the wash step was done, the final crystal was found by EPXMA to be free of Tl (spectrum D in Figure 1). One of these crystals (crystal 2) was sealed off for X-ray structure determination as before. If the wash step was omitted, the final crystal was found to have numerous black spots on its surface and EPXMA showed that it continued to contain Tl (spectrum C). This indicates that exposure of the pale yellow crystals (the product of the reaction of Tl−A with In) was sufficient to cause all residual Tl species to cluster to form black material, probably mostly on the zeolite surfaces. That these crystals remained black even after washing indicates that some black material remained on the crystal surfaces; any TlOH or $Tl(OH)_3$ (both soluble) should have washed away. That these crystals became colorless upon subsequent dehydration indicates that these black species, perhaps after having reacted further with oxygen or water, were volatile (Tl and/or Tl_2O). The black spots on the surface of the clear unwashed crystal are therefore attributed to Tl_2O_3, not volatile at 623 K, which formed upon dehydration from surface Tl species, such as $Tl(OH)_3$, which had not been washed away.

In^+ within the zeolite may have partially disproportionated upon initial hydration. This could have generated all of the In^{2+} and In^0 found in crystal 2 and some In^0 on the surface of the zeolite by the following reaction per unit cell: In^+_{12}−A → $In^+_8In^{2+}_2In^0$−A (crystal 2) + In^0 (surface). In^0 and any oxide (In_2O and/or In_2O_3) which may have formed are all black, and all could have left the zeolite upon further treatment as In_2O (volatile) or as hydroxides (soluble).

EPXMA of the above samples (A, B, C, and D) after exposure to the atmosphere were carried out with an EDAX 9100 system, an energy dispersive spectrometer (EDS) system attached to a Phillips 515 SEM.

Further EPXMA experiments using the fresh surface of an intentionally broken crystal of sample D confirmed that In is the only nonframework element present in the product. Its indium content was found semiquantitatively to be *ca.* 44 dry wt %, which corresponds to about 10 In atoms or ions/unit cell. This result is consistent with the later more precise crystallographic determination of 11 In species/unit cell.

Three space groups (*Pm*3*m*, *Fm*3*c*, and *Fm*3*m*)[43−45] were carefully considered for crystal 2. The cubic space group *Pm*3*m* (no systematic absences) was selected for use throughout this work for reasons described later in this section and for reasons discussed previously.[46,47] A CAD4/Turbo diffractometer equipped with a rotating anode generator and a graphite monochromator was used for preliminary experiments and for the subsequent collection of diffraction intensities, all at 294(1) K. Molybdenum radiation ($K\alpha_1$, λ = 0.709 30 Å; $K\alpha_2$, λ = 0.713 59 Å) was used. In each case, the cell constant, a = 12.153(4) and 12.098(2) Å for crystals 1 and 2, respectively, was determined by a least-squares treatment of 15 intense reflections for which $20 < 2\theta < 30°$. The $\omega-2\theta$ scan technique was used for data collection. Each reflection was scanned at a constant scan speed of 0.5°/min in 2θ with a scan width of $(0.50 + 0.61 \tan \theta)°$ and $(0.58 + 0.76 \tan \theta)°$, respectively, for crystals 1 and 2. Background intensity was counted at each end of a scan range for a time equal to half the scan time. The intensities of three reflections in diverse regions of reciprocal space were recorded every 3 h to monitor crystal and instrumental stability. Only small random fluctuations of these check reflections were observed during the course of data collection. The intensities of all lattice points (h,k,l) for which $h \le k \le l$ and $2\theta < 70°$ were recorded. This high upper limit for 2θ was chosen to give a more complete data set, even though few reflections with large 2θ values showed significant intensity.

For both crystals, the raw intensities were calculated by using procedures described before.[47,49] The observed structure factor amplitude of each reflection (F_o) was obtained as the square root of I_{raw} after correction for Lorentz/polarization. Standard deviations ($\sigma(F_o)$) of observed structure factors were assigned to individual reflections by the formula, $(\sigma^2(I) + (pF_o^2))^{1/2}/2F_o$, where $\sigma(I)$ is the standard deviation, based on counting statistics, of I_{raw}. The value p = 0.04 was found to be appropriate for the instrumentation used. Absorption corrections (μ = 27.5 and 3.89 mm^{-1} for crystals 1 and 2,[50] respectively) were judged to be negligible for both crystals. Only those reflections in each final data set for which the net count exceeded 3 times its standard deviation were used in structure solution and refinement. This amounted to 264 and 293 reflections for crystals 1 and 2, respectively.

Finally, crystal 2 was examined in the lower space group *Fm*3*c* which recognizes the silicon/aluminum ordering in the zeolite A framework.[43,44] Reflections (h,k,l) of the supercell (a = 24.188(3) Å) for which $h \le k \le l$ and $2\theta < 70°$ were gathered under the same conditions as before. Of 326 reflections for which the net count exceed 3 times its corresponding estimated standard deviation, 258 had even, even, even Miller indices and 68 were odd, odd, odd. Of the latter, 38 (more than half) were inconsistent with the space group *Fm*3*c*, violating its *c*-glide condition, affirming again the common observation that the ions and guests compromise the ideal symmetry of the zeolite framework severely. A test refinement with those reflections omitted were carried out for comparison with those of *Pm*3*m* (*vide infra*).

Structure Determination

Tl_{12}−A (Crystal 1). Full-matrix least-squares refinement[51] was initiated with the atomic parameters of all framework atoms [(Si,Al), O(1), O(2), and O(3)] and Tl^+ at Tl(1) in Tl^+-exchanged zeolite A.[36,37] The refinement with anisotropic thermal parameters for all framework atoms and an isotropic one for Tl(1) converged to the error indices $R_1 = \sum||F_o| - |F_c||/\sum F_o = 0.20$ and $R_2 = (\sum w(|F_o| - |F_c|)^2/\sum wF_o^2)^{1/2} = 0.28$ with an occupancy of 5.14(11) at Tl(1). Refinement with Tl(2) introduced at a peak ((0.105,0.105,0.105) inside the sodalite unit) found in a difference Fourier function prepared from this model converged to R_1 = 0.16 and R_2 = 0.22 with resulting occupancies of 4.97(8) and 1.04(8) at Tl(1) and Tl(2), respectively. A peak (0.0,0.434,0.5) found in a subsequent difference Fourier function was introduced at Tl(3). This model converged to the error indices R_1 = 0.075 and R_2 = 0.079, with occupancies of 6.91(4), 1.98(4), and 3.22(6) at Tl(i), i = 1−3, respectively. Lowering the symmetry at Tl(3) to (0,y,z) in subsequent refinement further reduced the error indices to R_1 = 0.063 and R_2 = 0.068 with occupancies of 6.90(4), 2.00(4), and 3.16(5) for isotropically refined Tl(i), i = 1−3, respectively. When the occupancies of all Tl^+ ions were fixed at their nearest integers (7.0, 2.0, and 3.0 (its maximum value due to packing

TABLE 1: Positional, Thermal, and Occupancy Parameters[a]

	Wyckoff position	*x*	*y*	*z*	β_{11}[b] or B_{iso}[c]	β_{22}	β_{33}	β_{12}	β_{13}	β_{23}	occupancy[d] fixed	occupancy[d] varied
					(a) Tl_{12}−A, Crystal 1							
(Si, Al)	24 (*k*)	0	1823(5)	3673(5)	11(3)	7(3)	5(3)	0	0	9(6)	24[e]	
O(1)	12 (*h*)	0	2044(20)	5000[f]	24(16)	50(17)	37(17)	0	0	0	12	
O(2)	12 (*i*)	0	3027(13)	3027(13)	12(12)	21(9)	21(9)	0	0	14(27)	12	
O(3)	24 (*m*)	1142(8)	1142(8)	3281(11)	21(6)	21(6)	28(11)	19(18)	28(13)	28(13)	24	
Tl(1)	8 (*g*)	2587(1)	2587(1)	2587(1)	35.3(4)	35.3(4)	35.3(4)	−4(2)	−4(2)	−4(2)	7	6.90(4)
Tl(2)	8 (*g*)	1029(4)	1029(4)	1029(4)	59(3)	59(3)	59(3)	−9(7)	−9(7)	−9(7)	2	2.00(5)
Tl(3)	24 (*k*)	0	4374(6)	4778(8)	146(10)	38(5)	56(11)	0	0	−23(12)	3	3.16(5)
					(b) In_{10}−A·In, Crystal 2							
(Si, Al)	24 (*k*)	0	1825(2)	3669(2)	20(2)	16(2)	13(2)	0	0	4(3)	24[e]	
O(1)	12 (*h*)	0	2022(10)	5000[f]	117(13)	76(11)	1(6)	0	0	0	12	
O(2)	12 (*i*)	0	3034(6)	3034(6)	41(8)	27(4)	27(4)	0	0	30(13)	12	
O(3)	24 (*m*)	1136(4)	1136(4)	3248(6)	43(4)	43(4)	59(7)	32(10)	−13(9)	−13(9)	24	
In(1)	8 (*g*)	2558(2)	2558(2)	2558(2)	2.50(5)						4	4.05(2)
In(2)	8 (*g*)	1314(2)	1314(2)	1314(2)	0.40(6)						2	2.01(2)
In(3)	8 (*g*)	1052(6)	1052(6)	1052(6)	2.5(3)						1	0.95(2)
In(4)	24 (*k*)	0	4318(10)	4710(11)	3.2(4)						1.5	1.40(3)
In(5)	24 (*l*)	601(18)	4142(18)	5000[f]	7.4(7)						1.5	1.58(4)
In(6)	1 (*a*)	0	0	0	0.8(1)						0.5	0.52(1)
In(7)	12 (*j*)	3054(30)	3054(30)	5000[f]	7.3(12)						0.5	0.49(3)

[a] Positional and anisotropic thermal parameters are given × 10^4. Values in parentheses are the estimated standard deviations in the units of the least significant figure given for the corresponding parameter. The anisotropic temperature factor is $\exp[-(\beta_{11}h^2 + \beta_{22}k^2 + \beta_{33}l^2 + \beta_{12}hk + \beta_{13}hl + \beta_{23}kl)]$. [b] Root mean square displacements can be calculated from β_{ii} values using formula $\mu_i = 0.225a(\beta_{ii})^{1/2}$, where $a = 12.153(4)$ and 12.098(1) Å for crystals 1 and 2, respectively. [c] Isotropic thermal parameter in units of Å^2. [d] Occupancy factors are given as the number of atoms or ions per unit cell. [e] Occupancy for Si = 12, occupancy for Al = 12. [f] Exactly 0.5 by symmetry.

considerations), respectively), the refinement converged with $R_1 = 0.064$ and $R_2 = 0.070$. Final cycles of refinement with anisotropic thermal parameters for all atoms quickly converged to $R_1 = 0.054$ and $R_2 = 0.060$. The final difference Fourier function was featureless. The final structural parameters are given in Table 1a. Selected interatomic distances and angles are given in Table 2.

In_{10}−A·In (Crystal 2). Full-matrix least-squares refinement began with the atomic parameters of all framework atoms [(Si,Al), O(1), O(2), and O(3)] in crystal 1 and In atoms at In(1) opposite 6-rings in large cavity (0.25,0.25,0.25), a most popular site for cations of medium size.[52,53] A refinement with anisotropic thermal parameters for all framework atoms in this model, with In(1) refining isotropically, converged to the error indices $R_1 = 0.31$ and $R_2 = 0.38$ with an occupancy of 2.21(1) at In(1). Introducing In(2) isotropically at a peak (0.125,0.125,0.125) from a difference Fourier function further reduced the error indices to $R_1 = 0.26$ and $R_2 = 0.33$ with resulting occupancies of 3.06(12) and 5.41(18) at In(1) and In(2), respectively. A refinement with the inclusion of In(4) isotropically at another peak (0.0,0.5,0.5) found in a difference function converged to $R_1 = 0.21$ and $R_2 = 0.25$ with resulting occupancies of 4.18(12), 3.57(13), and 2.14(13) at In(1), In(2), and In(4), respectively. The relatively large thermal parameter (33.5 Å^2) at In(4) suggested that the In species at In(4) was only near, rather than at, the highly symmetric (0.0,0.5,0.5) position. Isotropic refinement of a position with *m* (0,*y*,*z*) rather than the 4/*mmm* symmetry was successful with a reasonable thermal parameter of 6.0 Å^2 at In(4); this further reduced the error indices by a small amount to $R_1 = 0.21$ and $R_2 = 0.24$. A subsequent difference Fourier function based on this model revealed several peaks: (0.0,0.0,0.0), (0.058,0.416,0.5), and (0.313,0.313,0.5). A refinement with inclusion of the peak at origin (center of sodalite unit) at In(6) quickly converged to $R_1 = 0.12$ and $R_2 = 0.13$ with an occupancy of 0.47(2) at In(6). Inclusion of the other two peaks, (0.058,0.416,0.5) and (0.313,0.313,0.5), at In(5) and In(7) further reduced the error indices to $R_1 = 0.096$ and $R_2 = 0.093$ with resulting occupancies of 3.99(4), 2.78(4), 1.56(4), 1.47(6), 0.54(1), and 0.59(7) for In(i), i = 1, 2, and 4−7, respectively. Another peak was found in the ensuing difference Fourier function near In(2) on a threefold axis in the sodalite unit. Inclusion of this peak at In(3) in a subsequent refinement further reduced the error indices to $R_1 = 0.062$ and $R_2 = 0.061$, with resulting occupancies of 3.97(2), 1.91(2), 0.95(2), 1.36(3), 1.55(4), 0.52(1), and 0.49(4) at In(i), i = 1 to 7, respectively. All In positions were refined isotropically.

Considering the approach distances of all In species in this model (In(*i*), $i = 1-7$), the correct scattering factors of In^{2+} (In(2)), In^+ (In(1), In(3), In(4), and In(5)), and In^0 (In(6) and In(7), *vide infra*) were applied at this stage of refinement. This model converged to the error indices $R_1 = 0.061$ and $R_2 = 0.060$ with resulting occupancies of 4.05(2), 2.01(2), 0.95(2), 1.40(3), 1.58(4), 0.52(1), and 0.49(3) at In(*i*), $i = 1-7$, respectively. Applying anisotropic thermal parameters to each of the In positions led to no further decreases in the error indices. The final cycles of refinement were carried out with all In positions isotropic and occupancies fixed at 4.0, 2.0, 1.0, 1.5, 1.5, 0.5, and 0.5 at In(*i*), $i = 1-7$, respectively. This converged to the final error indices $R_1 = 0.063$ and $R_2 = 0.062$. The difference Fourier function based on this model was featureless. Final structural parameters are presented in Table 1b, and interatomic distances and angles are given in Table 2.

Refinement with *Fm*3*c* data sharply increased the error indices ($R_1 = 0.113$ and $R_2 = 0.126$) with non-positive-definite parameters for some framework atoms. Furthermore, the resulting crystallographic parameters yielded no additional information on the occupancies and geometries of the In species. Accordingly, this refinement was discontinued. Structural parameters and selected interatomic distances and angles resulted from the refinement in the space group *Fm*3*c* are given in Supporting Information Tables S1 and S2 for comparison. The space group *Fm*3*m*, which was reported to be appropriate for "K_5/K_{12}−A",[45] was also dismissed because the error indices could not be lowered below 0.23. Finally, extensive but unsuccessful efforts were made in the space group *F*43*m*, again in an attempt to find an ordered arrangement of In clusters.

For crystals 1 and 2, the values of the goodness-of-fit, ($\sum w$

TABLE 2: Selected Interatomic Distances (Å) and Angles (deg) of Tl_{12}−A and In_{10}−A·In[a]

(a) Tl_{12}−A		(b) In_{10}−A·In	
(Si,Al)−O(1)	1.635(8)	(Si,Al)−O(1)	1.629(3)
(Si,Al)−O(2)	1.660(18)	(Si,Al)−O(2)	1.652(7)
(Si,Al)−O(3)	1.685(11)	(Si,Al)−O(3)	1.686(5)
Tl(1)−O(3)	2.624(8)	In(1)−O(3)	2.573(4)
Tl(1)−O(2)	3.234(3)	In(1)−O(2)	3.201(2)
Tl(2)−O(3)	2.745(16)	In(2)−O(3)	2.359(8)
Tl(2)−O(2)	3.655(12)	In(2)−O(2)	3.345(5)
Tl(3)−O(1)	2.845(30)	In(3)−O(3)	2.661(11)
Tl(3)−O(2)	2.686(23)	In(3)−O(2)	3.622(7)
Tl(1)−Tl(2)	3.282(4)	In(4)−O(2)	2.554(14)
Tl(2)−Tl(2)	4.330(7)	In(4)−O(1)	2.800(17)
		In(5)−O(1)	2.666(25)
		In(5)−O(2)	2.825(13)
		In(6)−O(3)	4.384(7)
		In(6)−O(2)	5.192(5)
		In(7)−O(1)	3.900(35)
		In(7)−O(3)	3.907(22)
		In(2)−In(6)	2.754(2)
		In(3)−In(6)	2.205(5)
		In(1)−In(7)	3.073(8)
		In(4)−In(7)	4.014(34)
		In(5)−In(7)	3.247(40)
		In(7)−In(7)	3.330(37)
O(1)−(Si,Al)−O(2)	108.8(11)	O(1)−(Si,Al)−O(2)	109.3(5)
O(1)−(Si,Al)−O(3)	111.1(7)	O(1)−(Si,Al)−O(3)	111.8(4)
O(2)−(Si,Al)−O(3)	107.4(4)	O(2)−(Si,Al)−O(3)	107.3(2)
O(3)−(Si,Al)−O(3)	110.9(8)	O(3)−(Si,Al)−O(3)	109.2(3)
(Si,Al)−O(1)−(Si,Al)	161.1(20)	(Si,Al)−O(1)−(Si,Al)	163.2(9)
(Si,Al)−O(2)−(Si,Al)	146.5(10)	(Si,Al)−O(2)−(Si,Al)	145.4(4)
(Si,Al)−O(3)−(Si,Al)	136.9(9)	(Si,Al)−O(3)−(Si,Al)	135.7(5)
O(3)−Tl(1)−O(3)	89.0(5)	O(3)−In(1)−O(3)	89.2(2)
O(3)−Tl(2)−O(3)	84.1(3)	O(2)−In(1)−O(2)	108.4(1)
O(1)−Tl(3)−O(2)	53.0(3)	O(3)−In(2)−O(3)	100.0(1)
		O(2)−In(2)−O(2)	101.8(1)
		O(3)−In(3)−O(3)	85.6(2)
		O(2)−In(3)−O(2)	91.6(2)
		O(1)−In(4)−O(2)	59.7(3)
		O(1)−In(5)−O(2)	58.2(4)
		In(2)−In(6)−In(2)	109.4(3)
		In(1)−In(7)−In(1)	148.0(9)
		In(4)−In(7)−In(4)	135.2(6)
		In(1)−In(7)−In(4)	84.9(6)

[a] Values in parentheses are the estimated standard deviations in the units of the least significant digit given for the corresponding parameters.

$(F_o - |F_c|)^2/(m - s))^{1/2}$, are 1.73 and 1.69; the number of observations m are 261 and 293, and the number of parameters, s, are 33 and 36, respectively. All shifts in the final cycles of refinement for both crystals were less than 0.1% of their corresponding estimated standard deviations. The quantity minimized in least-squares is $\Sigma w(F_o - |F_c|)^2$, and the weights w are the reciprocal squares of $\sigma(F_o)$, the standard deviation of each observed structure factor. Scattering factors for Tl^+, In^{2+}, In^+, In^0, O^-, and $(Si,Al)^{1.75+}$ were used.[54,55] The functions used for In^{2+} and In^+ were calculated from those of In^{3+} and In^0 ($(2In^{3+} + In^0)/3$ and $(In^{3+} + 2In^0)/3$). The function describing $(Si,Al)^{1.75+}$ is the mean of the Si^{4+}, Si^0, Al^{3+}, and Al^0 functions. All scattering factors were modified to account for anomalous dispersion.[56,57]

Results and Discussion

Electron-Probe X-ray Microanalyses. The EPXMA experiments showed that the final product D is an indium aluminosilicate free of Tl. In all four spectra in Figure 1, the Kα lines of Al and Si appear consistently with almost the same relative intensities,[58] indicating that the composition of the zeolite framework was not modified by the reaction. The M_α and M_β lines (overlapping) of Tl in spectrum A (without those of In), and the L_α and L_β lines of In in spectrum D (without those of Tl),[58] indicate that the replacement of Tl^+ by In species is complete.

Tl^+ Ions in Tl_{12}−A (Crystal 1). In the crystal structure of fully dehydrated Tl_{12}−A, 12 Tl^+ ions/unit cell are distributed over three crystallographic positions. Nine of these Tl^+ ions are at two nonequivalent 3-fold-axis equipoints: seven at Tl(1) extend 1.54 Å into the large cavity from the O(3) planes of the six rings and two at Tl(2) are in the sodalite unit, 1.74 Å from these planes. These ions at Tl(1) and Tl(2) are trigonally coordinated by their respective sets of three O(3) framework oxygens at 2.624(8) and 2.745(16) Å, respectively (see Tables 1 and 2). Three additional Tl^+ ions per unit cell at Tl(3), to complete the total of 12 Tl^+ ions needed to balance the charge of the zeolite framework, are located in the planes of the 8-rings, 0.81 Å from their centers so as to make favorable approaches to the framework: 2.686(23) Å for Tl(3)−O(2) and 2.845(30) Å for Tl(3)−O(1).

The Tl(1) and Tl(2) positions are very much like those found in previous work,[36,37] while the position of Tl(3) on the eight rings is slightly different from, and better defined than, that found in some structures of partially and fully Tl^+-exchanged zeolite A.[36,37,61] The crystal of dehydrated Tl_{12}−A studied previously was prepared by using an ion-exchange solution of aqueous thallous hydroxide.[37] It differs from the present structure in the number of Tl^+ ions associated with six rings in the large cavity at Tl(1): six there and seven here. Unlike the previously reported Tl_{12}−A structure,[37] no 'near zero coordinate Tl^+ ion' is found deep in the large cavity in this work.

One of the eight 6-rings per unit cell must associate with two 3-fold-axis Tl^+ ions, Tl(1) in the large cavity and Tl(2) in the sodalite unit. Since the positions of these two Tl^+ ions must be somewhat different from those of the other Tl^+ ions at Tl(1) and Tl(2), extensive attempts were made to differentiate these two from the others by least-squares refinement; these were unsuccessful. These two Tl^+ ions, which share the same three O(3) framework oxygens of their 6-ring, should be somewhat more than the calculated distance of *ca.* 3.282(4) Å apart. Two Cs^+ ions similarly share a single 6-ring in the crystal structure of fully Cs^+-exchanged zeolite A.[28,29]

Indium Atoms and Ions in In_{10}−A·In (Crystal 2). In the crystal structure of In_{10}−A·In, 11 In atoms or ions/unit cell are distributed over seven crystallographic positions. The oxidation state at each position is identified on the basis of approach distances to framework atoms and each other. Seven In species per unit cell are found at three nonequivalent threefold-axis equipoints: four In^+ ions lie opposite 6-rings in the large cavity at In(1), and two In^{2+} at In(2) and one In^+ at In(3) lie opposite 6-rings in the sodalite unit. Three In^+ ions per unit cell are found at two different 8-ring positions: 1.5 In^+ ions at In(4) lie in an 8-ring plane, and 1.5 others at In(5) lie near this plane. Finally, one indium per unit cell, probably a neutral atom associated with In cations, is found at two quite unusual positions: one-half In^0 is at the center of the sodalite unit at In(6) and the other half In^0 lies opposite a 4-ring, relatively deep in large cavity at In(7).

(a) Monopositive Indium Ions. The four indiums at In(1) are each 2.573(4) Å from three 6-ring oxygens at O(3) (see Table 2). These indiums extend 1.50 Å into the large cavity from the (111) planes at O(3) (see Table 3). Considering the ionic radii of the framework oxygens to be 1.32 Å,[46,62,63] the radii of these indiums must be *ca.* 2.57−1.32 = 1.25 Å. This is somewhat shorter than those found for In^+, which range from 1.32 to 1.51 Å in various indium halides.[64−66] However,

TABLE 3: Deviations of Atoms (Å) from the (111) Plane at O(3)[a]

crystal	cation	charge	distance
Tl_{12}−A (crystal 1)	Tl(1)	+1	1.54
	Tl(2)	+1	−1.74
In_{10}−A·In (crystal 2)	In(1)	+1	1.50
	In(2)	+2	−1.10
	In(3)	+1	−1.65
	In(6)	0	−3.86[b]

[a] A negative deviation indicates that the ion lies on the same side of the plane as the origin, *i.e.*, inside the sodalite unit. [b] Located at the origin, the center of the sodalite unit.

similarly shortened radii have been found for Tl^+ ions in zeolites; *ca.* 1.30 Å *vs ca.* 1.47 Å in various thallous halides, respectively,[36,37,61] probably due to the low coordination number of these ions in the dehydrated zeolite. An even smaller radius, 1.17 Å, was suggested for In^+ by a theoretical calculation using the numerical HF method.[67] Accordingly, the oxidation state of the indiums at In(1) appears to be 1+.

Three similar In^+ ions per unit cell are found at In(4) and In(5). The 1.5 In^+ ions at In(4) are 2.554(14) Å from O(2) 8-ring oxygens, showing a very similar radius of *ca.* 1.23 Å. The 1.5 In^+ ions at In(5) are 2.666(25) Å from the O(1) oxygens. The latter somewhat longer distance can probably be attributed to differences in environment: approach distances of monopositive cations to 8-ring oxygens are commonly longer than those to 6-ring oxygens in zeolite A.[28,29,36,37,43,48,61]

The indium at In(3) is also judged to be an In^+ ion. Its approach distances to the nearest 6-ring oxygens, three O(3)s, are 2.661(11) Å. This is also somewhat longer than the corresponding In^+ ions at In(1). Again, such a difference is commonly seen for many cations located in the sodalite unit.[28,29,36,37] Considering further that the total cationic charge per unit cell should be 12+ (*vide infra*), the indium at In(3) should be In^+.

(b) Dipositive Indium Ions. The two indiums per unit cell at In(2) are found to be sharply closer to the 6-ring oxygens than any other indiums in this structure, and so do not appear to be In^+. They approach three O(3) 6-ring oxygens at 2.359(8) Å. They therefore have an ionic radius of *ca.* 1.04 Å (2.36−1.32 Å), and so must have a higher oxidation state, probably 2+, than the In^+ ions at In(*i*), $i = 1$, 3, 4, and 5. The ionic radius of 1.04 Å for the In^{2+} at In(2) is somewhat longer than the average value, 0.95 Å, of the ionic radii of the adjacent cations in periodic table, Cd^{2+} (0.97 Å) and Sn^{2+} (0.93 Å).[62,63] This is probably because of the reduced cationic character at In(2) due to association with the In^0 atoms at the center of the sodalite unit (*vide infra*). These In^{2+} ions must be the result of the disproportionation of In^+ ions, *i.e.* $2In^+ \rightarrow In^{2+} + In^0$, upon exposure of the reacted crystal to the atmosphere, as evidenced by the migration of In^0 out to the crystal surface. This is the first identification of relatively isolated In^{2+} ions; In^{2+} had been seen before in some indium trihalide dimers such as $[In_2Cl_6]^{2-}$.[68,69]

(c) Indium Atoms. The indiums at In(6) and In(7), amounting to just one indium per unit cell at two crystallographically distinct positions (0.5 at In(6) at the center of the sodalite unit and 0.5 at In(7) opposite a 4-ring deep in the large cavity) make no close approaches to any framework atoms. However, they are reasonably close to indium cations both in the sodalite unit and in the large cavity, suggesting that they are In atoms (In^0) bound to cations.

These assignments of cationic charges (sections a, b, and c above) sum to a total charge of 12+ per unit cell, correctly balancing the charge of the zeolite A framework.

(d) Indium Clusters. The location of In^0 at In(6), at the center of the sodalite unit, is unambiguous, because no other chemically possible atom or ion, such as Al or O which might have been produced during the reactions between In^0 and Tl_{12}−A and/or introduced during later exposure to air or water, could account for the electron density (*ca.* 23 electrons) found at this special position. An impossibly short approach distance of 2.205(5) Å between indiums at In(3) and In(6) in the same sodalite unit is found and is avoided in the structure proposed. However, In^0 at In(6) is 2.754(2) Å from In^{2+} at In(2). This is a reasonable bonding distance for In^0−In^{2+}, considering that the sum of atomic and ionic radii of In^0 and In^{2+} is 2.67 (or 2.71) Å = 1.63 (or 1.67) + 1.04 Å.[70] The association of In^0 at In(6) with In(2) explains the rather longer approach distances of In^{2+} at In(2) to the 6-ring oxygens, due to the reduced cationic character of In^{2+} (*vide supra*). This reasonable inter-indium distance between In^0 and In^{2+} suggests the possibility of having clusters such as $(In_2)^{2+}$, $(In_3)^{4+}$ (linear or bent), or $(In_5)^{8+}$ (four In^{2+} ions tetrahedrally arranged in the sodalite unit with an In^0 at their center).

With a partial occupancy of 0.5 at In(6), the presence of $(In_2)^{2+}$ or $(In_3)^{4+}$ would require other unit cells to have nonequivalent In^{2+} ions at In(2), averaging to 2.0/sodalite unit as shown in Table 1b. However, differentiation of these two kinds of In^{2+} ions at In(2) was impossible crystallographically and is not suggested by the small thermal parameter at In(2), 0.4 Å^2. This and packing considerations for the indium species (*vide infra*), and the requirement for a relatively even distribution of cationic charges in various unit cells, strongly suggest that the most plausible cluster associated with In^0 at In(6) is the highly symmetric $(In_5)^{8+}$ cluster with inter-indium distances of 2.754(2) Å between each of the four In^{2+} ions at In(2) and the In atom at In(6) (their center) (see Figure 2). Similarly prepared In−A crystals treated with sulfur gas always show an In(2):In(6) ratio of 4:1, and the higher occupancy of 0.75 has been observed for $(In_5)^{8+}$.[71]

The other In^0 at In(7) deep in the large cavity probably associates with In^+ ions at In(1) or In(5). Of the two possible inter-indium distances, In(7)−In(1) distance = 3.073(8) Å and In(7)−In(5) distance = 3.247(40) Å, only the shorter is acceptable. Considering the sum of the ionic and atomic radii, 2.92 Å = 1.25 (r_{In^+}) + 1.67 Å (r_{In^0}), and the inter-indium distances of 2.754(2) Å for In^{2+}−In^0, the most plausible cluster is $(In_3)^{2+}$, In(1)−In(7)−In(1), with distances of 3.073(8) Å for In^+−In^0 and an angle of 148.0(9)° (see Figure 3).

(e) Arrangement of In Species in In_{10}−A·In. With ten cationic indiums (two In^{2+} and eight In^+ ions) at five distinct positions and one In^0 at two positions per unit cell, the unit cell formula may be written as $(In^{2+})_2(In^+)_8Si_{12}Al_{12}O_{48}$·In, or $(In^{2+})_2(In^+)_8$−A·In, or In_{10}−A·In. However, because some of the indiums cannot coexist in the same unit cell (for example, the indiums at In(3) and In(6) are impossibly close to each other), the structure found for In_{10}−A·In should be the average of two (or more) different unit cells or cavities with different indium contents.

The occupancy of 0.5 at In(6), because the maximum occupancy at this position per sodalite unit is 1, indicates that there are two kinds of sodalite cavities: one containing an In(6) atom at the center of $(In_5)^{8+}$ cluster and the other without one. Similarly, the existence of different large cavities in In_{10}−A·In is suggested by the existence of two crystallographically distinct In^+ positions at In(4) and In(5) about the 8-rings, with no noticeable difference in their immediate environments except for those which could result from different indium structure in adjacent large cavities and sodalite units. Moreover, the nonintegral occupancies of these In^+ ions, 1.5/unit cell for each, again strongly suggests two kinds of large cavities: one

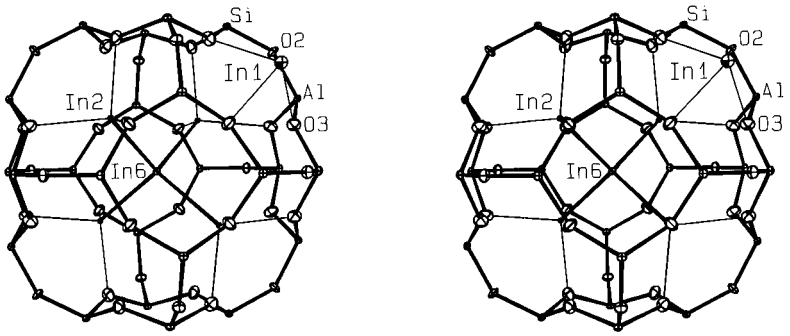

Figure 2. A stereoview of a sodalite unit in $In_8-A\cdot In$ (unit cell 1), showing an $(In_5)^{8+}$ cluster in its center. The zeolite A framework is drawn with solid bonds between tetrahedrally coordinated (Si and Al) and oxygen atoms. The bonds between the cationic In species and framework oxygens are indicated by fine solid lines. Bonds within the cluster are solid. Ellipsoids of 20% probability are shown.

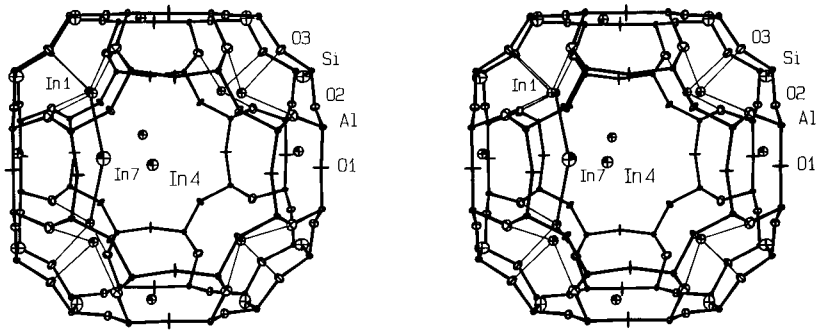

Figure 3. A stereoview of the large cavity of $In_{12}-A\cdot In$ (unit cell 2), showing an $(In_3)^{2+}$ cluster opposite a four-ring. See the caption to Figure 2 for other details.

TABLE 4: Distribution of In Species in Component "Unit Cells" of $In_{10}-A\cdot In$

indium species	position	charge	$In_8-A\cdot In$, unit cell 1		$In_{12}-A\cdot In$, unit cell 2		total (averaged)	
			no.	charge	no.	charge	no.	charge
			(a) as Individual Ions or Atoms					
In(1)	opposite 6-ring[a,b]	+1	1	+1	7	+7	4	+4
In(2)	opposite 6-ring[b,c]	+2	4	+8	0	0	2	+4
In(3)	opposite 6-ring[b,c]	+1	0	0	2	+2	1	+1
In(4)	8-ring[d]	+1	0	0	3	+3	1.5	+1.5
In(5)	8-ring[e]	+1	3	+3	0	0	1.5	+1.5
In(6)	origin[c,f]	0	1	0	0	0	0.5	0
In(7)	opposite 4-ring[a]	0	0	0	1	0	0.5	0
sum			9	+12	13	+12	11	+12
			(b) as Monatomic and Polyatomic Cations					
$(In_5)^{8+}$	In(2), In(6)	+8	1	+8	0	0	0.5	+4
$(In_3)^{2+}$	In(1), In(7)	+2	0	0	1	+2	0.5	+1
In^+	In(1)	+1	1	+1	5	+5	8	+3
In^+	In(3)	+1	0	0	2	+2	1	+1
In^+	In(4)	+1	0	0	3	+3	1.5	+1.5
In^+	In(5)	+1	3	+3	0	0	1.5	+1.5
sum			5	+12	11	+12	8	+12

[a] In the large cavity. [b] On 3-fold axes. [c] In the sodalite unit. [d] On the 8-ring plane. [e] Off the 8-ring plane. [f] At the origin; at the center of sodalite unit.

containing three In^+ ions at In(4) and the other with three at In(5). The crystal structure of $In_{10}-A\cdot In$ may, therefore, be best viewed as having two kinds of unit cells.

On the basis of these considerations, the mono- and polyatomic cations were placed within alternating unit cells following two criteria: (1) that the total cationic charge be 12+ for each unit cell, if possible, to balance best the anionic charge of the zeolite framework, and (2) that intercationic repulsions, especially these involving the highly charged $(In_5)^{8+}$ clusters, be minimized. Rather easily, the following unit cell formulas emerged: $(In^{2+})_4(In^+)_4-A\cdot In$ and $(In^+)_{12}-A\cdot In$ for unit cells 1 and 2, respectively. This nomenclature may be abbreviated to $In_8-A\cdot In$ and $In_{12}-A\cdot In$, respectively. The compositions and distribution of various In species in the two kinds of unit cells, each of which has a total cationic charge of 12+, are tabulated in Table 4.

$In_8-A\cdot In$ (unit cell 1) contains eight In^{n+} cations and one In^0 distributed over four crystallographically distinct positions: one In^+ ion at In(1) opposite 6-rings in the large cavity, four In^{2+} at In(2) opposite 6-rings in the sodalite unit, three In^+ at In(5) near the 8-rings, and finally one In^0 at In(6) at the center of the sodalite unit. Each $In_8-A\cdot In$ unit cell contains an $(In_5)^{8+}$ cluster inside its sodalite unit. The In^+ ions at In(5) appear to have moved off their 8-ring planes to distance themselves from this highly charged indium cluster. Stereoviews of a sodalite unit and of a large cavity of unit cell 1 are shown in Figures 2 and 4, respectively.

In $In_{12}-A\cdot In$ (unit cell 2), 12 In^+ ions and 1 In^0 are distributed

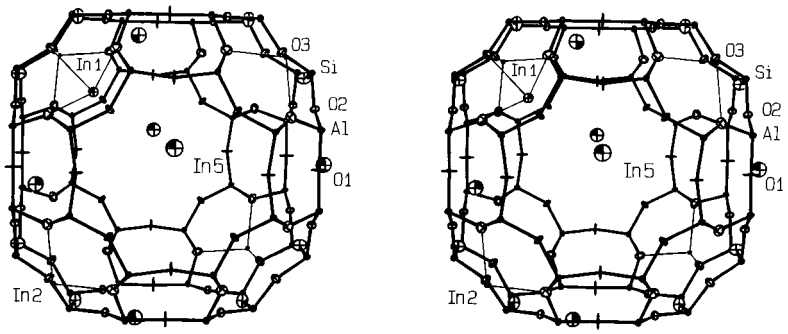

Figure 4. A stereoview of the large cavity of $In_8-A\cdot In$ (unit cell 1). See the caption to Figure 2 for other details.

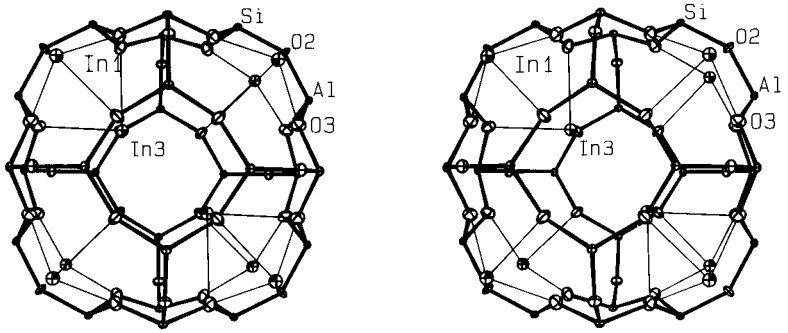

Figure 5. A stereoview of a sodalite unit of $In_{12}-A\cdot In$ (unit cell 2). See the caption to Figure 2 for other details.

over 4 distinct positions: 7 In^+ ions at In(1) opposite 6-rings in the large cavity, 3 In^+ at In(4) on the plane of 8 rings, two In^+ at In(3) opposite 6 rings in the sodalite unit, and finally 1 In^0 at In(7) opposite a 4-ring and deep in large cavity. In this arrangement, two In^+ ions, one at In(1) and the other at In(3), should share a 6-ring on a single 3-fold axis. A similar arrangement is also seen in $Tl_{12}-A$ (crystal 1). The bent $(In_3)^{2+}$ cluster is found in the large cavity of $In_{12}-A\cdot In$. Stereoviews of a sodalite unit and of a large cavity of unit cell 2 are shown in Figures 5 and 3, respectively.

Summary

Despite the small or negative values of ΔE°_{aq} for the reactions between Tl^+ and In^0,[32] the reaction $(Tl^+)_{12}-A + 11In^0 \rightarrow (In^{2+})_2(In^+)_8-A\cdot In + 12Tl^0$ has occurred. This reaction may include some disproportionation of In species which may have occurred upon exposure to the atmosphere. Perhaps the intrazeolitic reaction between Tl^+ and In^0 occurred because of mass action, or because of free energy changes due to temperature, but the clearest reason may be the favorable difference in ionization potential[33] between gaseous Tl^0 and In^0 for the reaction, $Tl^+ + In^0 \rightarrow In^+ + Tl^0$.

On the basis of the unambiguous results obtained from microanalysis, extended by the determination of the crystal structure of $In_{10}-A\cdot In$, it is clear that all Tl^+ ions in Tl−A have been replaced by In species due to reaction between the Tl^+ and In^0. The only cations or guests in the resulting zeolite (In−A) are monatomic and polyatomic indium cations. The unit cell formula of the product, $In_{10}-A\cdot In$, may be written as $[(In_5)^{8+}]_{0.5}[(In_3)^{2+}]_{0.5}(In^+)_7-A$, which is composed of two different "unit cells," both neutral, of composition $(In_5)^{8+}$-$(In^+)_4-A$ and $(In_3)^{2+}(In^+)_{10}-A$.

Further work on the chemical modification of In−A and on the characterization of the resulting products is in progress.

Acknowledgment. N. H. Heo gratefully acknowledges the support from the Central Laboratory of Kyungpook National University for the diffractometer and computing facilities. This work was supported in part by the Ministry of Education of Korea (Grant 01-D-0048).

Supporting Information Available: Comparison of least-squares refinement results in space groups *Pm*3*m* and *Fm*3*c* for $In_{10}-A\cdot In$ (parameters and geometry) and observed and calculated structure factors for fully dehydrated $Tl_{12}-A$ and $In_{10}-A\cdot In$ (10 pages). Ordering information is given on any current masthead page.

References and Notes

(1) Srdanov, V. I.; Blake, N. P.; Markgraber, D.; Metiu, H.; Stucky, G. D. *Advanced Zeolite Science and Applications, Studies in Surface Science and Catalysis;* Jansen, J. C., Stocker, M., Karge, H. G., Weitkamp, J., Eds.; Elsevier Science: Amsterdam, 1994; Vol. 85, pp 115−144.

(2) Terasaki, O.; Yamazaki, K.; Thomas, J. M.; Ohsuna, T.; Watanabe, D.; Sanders, J. V.; Barry, J. C. *Nature* (*London*) **1987**, *330*, 58−60.

(3) Stucky, G. D.; MacDougall, J. E. *Science* **1990**, *247*, 669−678.

(4) Moller, K.; Bein, T.; Herron, N.; Mahler, W.; Macdougall, J.; Stucky, G. D. *Mol. Cryst. Liq. Cryst.* **1990**, *181*, 305−314.

(5) Ozin, G. A.; Ozkar, S.; Prokopowicz, R. A. *Acc. Chem. Res.* **1992**, *25*, 553−560.

(6) Alekseev, Yu. A.; Bogomolov, V. N.; Zhukova, T. B.; Petranovskii, V. P.; Romanov, S. G.; Kholodkevich, S. V. *Izv. Akad. Nauk SSSR, Ser. Fiz.* **1986**, *50*, 418−423.

(7) Wang, Y.; Herron, N. *J. Phys. Chem.* **1987**, *91*, 257−260.

(8) Stramel, R. D.; Thomas, J. K. *J. Chem. Soc., Faraday Trans. 1*, **1988**, *84*, 1287−1300.

(9) Wang, Y.; Herron, N. J. *J. Phys. Chem.* **1988**, *92*, 4988−4994.

(10) Nozue, Y.; Tang, Z. K.; Goto, T. *Solid State Commun.* **1990**, *73*, 531−534.

(11) Herron, N.; Wang, Y.; Eddy, M. M.; Stucky, G. D.; Cox, D. E.; Moller, K.; Bein, T. *J. Am. Chem. Soc.* **1989**, *111*, 530−540.

(12) Kitagawa, H.; Sendoda, Y.; Ono, Y. *J. Catal.* **1986**, *101*, 12−18.

(13) Gnep, N. S.; Doyemet, J. Y.; Seco, A. M.; Ramoa, R. F.; Guisnet, M. *Appl. Catal.* **1988**, *43*, 155−166.

(14) Kanazirev, V.; Price, G. L.; Dooley, K. M. *Zeolite Chemistry and Catalysis*; Jacobs, P. A., Ed.; Elsevier: Amsterdam, 1991; pp 277−285.

(15) Mowry, J. R.; Anderson, R. F.; Johnson, J. A. *Oil Gas J.* **1985**, 128−131.

(16) Kanazirev, V.; Price, G. L.; Dooley, K. M. *J. Chem. Soc., Chem. Commun.* **1990**, 712−713.

(17) Price, G. L.; Kanazirev, V. *J. Catal.* **1990**, *126*, 267−278.

(18) Kanazirev, V.; Valtchev, V.; Tarassov, M. P. *J. Chem. Soc., Chem. Commun.* **1994**, 1043−1044.

(19) Alekseev, Yu. A.; Bogomolov, V. N.; Egorov, V. A.; Petranovskii, V. P.; Kholodkevich, S. V. *JETP Lett*. **1982**, *36*, 463−465.
(20) Alekseev, Yu. A.; Bogomolov, V. N.; Zhukova, T. B.; Petranovskii, V. P.; Kholodkevich, S. V. *Sov. Phys. Solid State* **1982**, *24* (8), 1384−1388.
(21) Uchida, H.; Ogata, T.; Yoneyama, H. *Chem. Phys. Lett*. **1990**, *173*, 103−106.
(22) Heo, N. H.; Choi, H. C. Unpublished results.
(23) Ashraf, M.; Aziz-Alrahmam, A. M.; Headbridge, J. B. *J. Chem. Soc. Dalton Trans.* **1977**, 170−173.
(24) Biedermann, G.; Wallin, T. *Acta Chem. Scand.* **1960**, *14*, 594−608.
(25) Thiel, A. *Z. Anorg. Chem.* **1904**, *40*, 280.
(26) Taylor, R. S.; Sykes, A. G. *J. Chem. Soc. A* **1969**, 2419−2423.
(27) Headridge, J. B.; Pletcher, D. *Inorg. Nuclear Chem. Letters* **1967**, *3*, 475−478.
(28) Heo, N. H.; Seff, K. *J. Am. Chem. Soc*. **1987**, *109*, 7986−7992.
(29) Heo, N. H.; Seff, K. In *Perspectives in Molecular Sieve Science;* ACS Symposium Series 368; Flank, W. H., Whyte, T. E., Jr., Eds.; American Chemical Society: Washington, DC, 1988; pp 177−193.
(30) Sun, T.; Seff, K. *J. Phys. Chem.* **1993**, *97*, 5213−5214.
(31) Blackwell, C. S.; Pluth, J. J.; Smith, J. V. *J. Phys. Chem*. **1985**, *89*, 4420−4423.
(32) *Handbook of Chemistry and Physics*, 74th ed.; Chemical Rubber Co.: Cleveland, OH, 1993; pp 8−23.
(33) Emsley, J. *The Elements*, 2nd ed.; Clarendon Press: Oxford, 1991; pp 90, 192.
(34) The nomenclature refers to the contents of the *Pm*3*m* unit cell, *e.g.*, Na_{12}−A represents $Na_{12}Si_{12}Al_{12}O_{48}$ and Tl_{12}−A represents $Tl_{12}Si_{12}Al_{12}O_{48}$.
(35) Charnell, J. F. *J. Cryst. Growth* **1971**, *8*, 291−294.
(36) Riley, P. E.; Seff, K.; Shoemaker, D. P. *J. Phys. Chem*. **1972**, *76*, 2593−2597.
(37) Firor, R. L.; Seff, K. J. *Am. Chem. Soc*. **1977**, *99*, 4039−4044.
(38) Wade, K.; Banister, A. J. *Comprehensive Inorganic Chemistry;* Bailar, J. C., Jr., Ed.; Pergamon Press, Oxford, 1973; Vol. 1, pp 997−1000.
(39) Barin, I. *Thermochemical Data of Pure Substances*; VCH: Weinheim, 1989; Part I, p 716.
(40) Reference 32, pp 4−63.
(41) Reference 32, pp 6−89.
(42) Cubicciotti, D. *High Temp. Sci.* **1970**, *2*, 213. Rat'kovskii, I. A.; Semenov, G. A. *Chem. Abstr*. **1970**, *73*, 39384k. The formula in the latter reference should be $\log p = A - B/T$.
(43) Gramlich-Meier, R.; Gramlich, V. *Acta Crystallogr., Sect. A* **1982**, *38*, 821−825.
(44) McCusker, L. B.; Seff, K. *J. Am. Chem. Soc.* **1981**, *103*, 3441−3446.
(45) Armstrong, A. R.; Anderson, P. A.; Edwards, P. P. *J. Chem. Soc., Chem. Commun.* **1994**, 473−474.
(46) Cruz, W. V.; Leung, P. C. W; Seff, K. *J. Am. Chem. Soc.* **1978**, *100*, 6697−7003.
(47) Mellum, M. D.; Seff, K. *J. Phys. Chem*. **1984**, *88*, 3560−3563.
(48) Heo, N. H.; Cho, K. H.; Kim, J. T.; Seff, K. *J. Phys. Chem*. **1994**, *98*, 13328−13333.
(49) Cho, K. H.; Kwon, J. H.; Kim, H. W.; Park, C. S; Heo, N. H. *Bull. Korean Chem. Soc.* **1994**, *15*, 297−304.
(50) *International Tables for X-ray Crystallography;* Ibers, J. A., Hamilton, W. C., Eds.; Kynoch Press: Birmingham, England, 1974; Vol. IV, pp 61−66.
(51) Calculations were performed with *Structure Determination System MolEN*; Enraf-Nonius: The Netherlands, 1990.
(52) Leung, P. C. W.; Kunz, K. B.; Maxwell, I. E.; Seff, K. *J. Phys. Chem.* **1975**, *79*, 2157−2162.
(53) Firor, R. L.; Seff, K. *J. Am. Chem. Soc.* **1977**, *99*, 1112−1117.
(54) Doyle, P. A.; Turner, P. S. *Acta Crystallogr., Sect. A* **1968**, *24*, 390−397.
(55) Reference 50, pp 73−87.
(56) Cromer, D. T. *Acta Crystallogr*. **1965,** *18*, 17−23.
(57) Reference 50, pp 149−150.
(58) Reference 32, pp 10−258.
(59) *Merck Index*, 11th ed.; Merck & Co.: Rahway, NJ, **1989**; pp 1458−1459.
(60) Kanazirev, V.; Neinska, Y.; Tsoncheva, T.; Kosova, L. In *Proceedings of the 9th International Zeolite Conference*, Montreal, 1992; Ballmoos, R. V., Higgins, J. B., Treacy, M. M. J., Eds.; Butterworth: Boston, 1993; Vol. 1, 461−468.
(61) Kim, Y.; Seff, K. *J. Phys. Chem*. **1978**, *82*, 1307−1311.
(62) *Handbook of Chemistry and Physics*, 64th ed; Chemical Rubber Co.: Cleveland, OH, 1983; p F-187.
(63) Shannon, R. D.; Prewitt, C. T. *Acta Crystallogr., Sect. B* **1969**, *25*, 925−946.
(64) Brode, H. *Ann. Phys.* **1940**, *37*, 344.
(65) Barrett, A. H.; Mandel, M. *Phys. Rev*. **1955**, *99*, 666.
(66) Barrow, R. F.; Glaser, D. V.; Zeeman, P. B. *Proc. Phys. Soc., London, Sect. A* **1955**, *68*, 962−968.
(67) Fraga, S.; Saxeua, K. M. S.; Karwowski, J. *Handbook of Atomic Data*; Elsevier Scientific: Amsterdam, 1976; p 465.
(68) Stevenson, D. P.; Schomaker, V. *J. Am. Chem. Soc*. **1942**, *64*, 2514−2514.
(69) Cotton, F. A.; Wilkinson, G. *Advanced Inorganic Chemistry*, 5th ed.; John Wiley & Sons, Inc.: New York, 1988; pp 209−233.
(70) Tyzack, G.; Raynor, G. V. *Trans. Faraday Soc.* **1954**, *50*, 675−68.
(71) Heo, N. H.; Kim, S. H.; Choi, H. C.; Seff, K. *J. Phys. Chem*. Submitted for publication.